www.e-kjar.org
https://doi.org/10.52668/kjar.2023.00024
pISSN 2586-1719 / eISSN 2799-3299

Korean J Abdom Radiol 2023;7:35-45

Original Article

Can Perfusion CT Differentiate GIST from Other Benign Subepithelial Tumors in the Stomach?

Seungchul Han[1], Se Hyung Kim[2,3], Dong Ho Lee[2,3]
[1]Department of Radiology, Samsung Medical Center, Seoul, Korea
[2]Department of Radiology, Seoul National University Hospital, Seoul, Korea
[3]Institute of Radiation Medicine, Seoul National University Medical Research Center, Seoul, Korea

Purpose: To evaluate the diagnostic performance of perfusion computed tomography (PCT) parameters for differentiating gastrointestinal stromal tumors (GISTs) from other benign subepithelial tumors (SETs) in the stomach.
Materials and Methods: Thirty-one patients with gastric SETs subsequently confirmed via surgery underwent PCT using a multidetector computed tomography (CT) scanner at 80 kVp. Two radiologists analyzed key CT features including homogeneity and degree of enhancement. PCT parameters including blood flow, blood volume, mean transit time, and permeability surface value (PS) were independently calculated by two other radiologists. Comparative analysis of the CT features and perfusion parameters of GISTs and other benign SETs was then performed. Diagnostic performances of the perfusion parameters were also evaluated using receiver operating characteristic (ROC) analysis.
Results: Twenty-four patients were proven to have GISTs via histologic examination, while the remaining non-GISTs included 3 leiomyomas, 3 schwannomas, and 1 totally necrotic nodule. Among the conventional CT features, lymphadenopathy was more frequent in non-GISTs (2/7, 28.6%) than in GISTs (0/24, 0%) ($p = 0.045$). Among the PCT parameters, the mean PS in the areas of strongest enhancement of GISTs (25.3 ± 23.9 mL/100 g/min) was significantly higher than that of other SETs (8.8 ± 8.8 mL/100 g/min) ($p = 0.029$). In ROC analysis, an area under the curve of 0.774 ($p = 0.03$), sensitivity of 91.7%, and specificity of 57.1% were achieved when the PS cut-off was set at 7.17 mL/100 g/min.
Conclusions: Perfusion parameters were helpful for differentiating GISTs from other benign SETs, as GISTs exhibited significantly higher PS than non-GISTs.

Keywords: Stomach; Gastrointestinal stromal tumors; Leiomyoma; Perfusion imaging; Task perfomance and analysis

Introduction

Although gastric subepithelial tumors (SETs) are considered "rare", they are quite frequently detected incidentally during esophagogastroduodenoscopy (1, 2). Gastric SETs include a wide variety of benign,

Received: April 27, 2023 **Revised:** June 19, 2023 **Accepted:** June 21, 2023
Correspondence: Se Hyung Kim, MD, PhD
Department of Radiology, Seoul National University Hospital and Seoul National University College of Medicine, 101 Daehakro, Jongno-gu, Seoul, 03080, Korea
Tel: +82-2-2072-2057 Fax: +82-2-743-6385 E-mail: shkim71@snu.ac.kr

premalignant, and malignant lesions. They can be classified into four main subtypes according to their origin; true smooth muscle tumors (leiomyomas, leiomyosarcomas, glomus tumors), neurogenic tumors (schwannomas, neurofibromas, ganglioneuromas, paragangliomas), fibroblastic tumors (desmoid, inflammatory myofibroblastic tumors), and gastrointestinal stromal tumors (GISTs) (3). With the exception of very rare leiomyosarcomas, all gastric mesenchymal tumors other than GISTs are almost always benign. GISTs however—even when they are small—are potentially malignant (4, 5). Therefore, accurate differentiation of GISTs from other benign SETs is crucial for management planning and predicting prognoses.

According to several previous reports, computed tomography (CT) findings including non-cardial location, heterogeneous enhancement, presence of necrosis, larger lesion size, and absence of lymphadenopathy are highly suggestive of large GISTs (≥ 5 cm), as opposed to schwannomas or leiomyomas (3, 6, 7). GISTs can sometimes manifest as well-defined masses with homogenous low attenuation in the cardial area, particularly if they are small (< 5 cm), rendering differentiation from leiomyoma or schwannoma challenging.

Advances in multidetector CT have resulted in the development of perfusion CT (PCT) as an attractive imaging modality that can determine tissue perfusion characteristics in various types of solid organ and hollow viscus tumors (8-11). Several recent studies have reported that PCT of gastric cancer is feasible, and gastric cancer perfusion parameters obtained from PCT data provide information on tumor vascularity and angiogenesis, making histologic differentiation and treatment monitoring with PCT possible (11-13). However, the differentiation of GISTs from other benign SETs using tumor perfusion parameters obtained via PCT has not been investigated. In the current prospective study, we investigated whether the perfusion parameters of gastric SETs obtained via PCT could provide useful information for differentiating between GISTs and non-GISTs in the stomach.

Materials and Methods

This prospective observational study included patients suspected of having gastric SETs attending an academic medical center from December 2017 to July 2018. The study was compliant with the Health Insurance Portability and Accountability Act and was approved by the appropriate institutional review board. Written informed consent was obtained from all subjects.

Study population

Fifty patients with a clinically suspected gastric SET greater than 1 cm in size as determined via endoscopy or incidental CT scanning were prospectively recruited at our institute. All patients underwent PCT. Of the 50 patients, 35 gastric SETs were pathologically confirmed via surgery (n = 34) or endoscopic resection (n = 1). Of these 35 patients, 4 with insufficient coverage of the tumor in dynamic scanning were excluded, therefore a total of 31 patients were ultimately included in further image analyses (Fig. 1). They consisted of 5 men and 26 women, with a mean age of 60.8 years (range 27–85 years). Twenty-nine underwent gastric wedge resection, and the remaining 2 underwent subtotal gastrectomy.

CT protocols

CT scans were performed with a 64-channel multidetector CT scanner (SOMATOM Definition, Siemens Healthcare, Forchheim, Germany). Before CT scanning, all patients were asked to drink 1 L of water to distend the stomach. No anti-peristaltic agent was used. After a baseline non-enhanced scan covering the distended

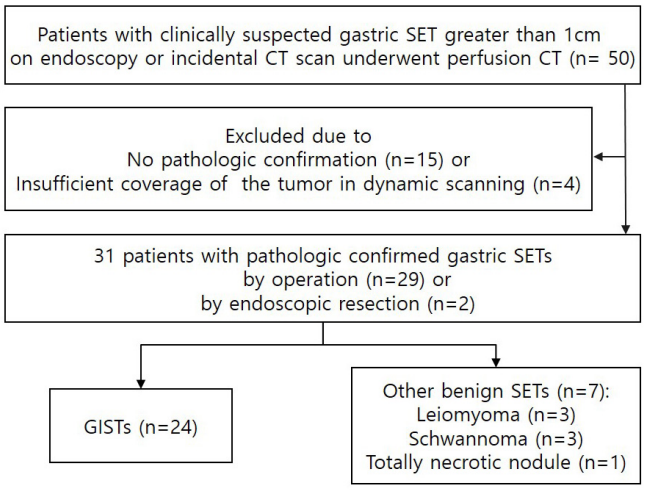

Fig. 1. Flow chart of study population. SET=subepithelial tumor, CT=computed tomography, GIST=gastrointestinal stromal tumor.

stomach, which was identified on a topogram, dynamic scanning for the target gastric lesion with a limited scanning range of 17.6 cm was conducted. In each patient, 50 mL of iodinate contrast agent (Bonorex 350; Central Medical Service, Seoul, Korea) was injected into an antecubital vein at a flow rate of 5 mL/sec followed by 50 mL of saline at the same flow rate. Seven seconds after the injection of contrast material, 15 spiral acquisitions were performed in four-dimensional spiral mode with a variable pitch. Images were acquired with a scanning time of 1.5 sec per spiral and a cycle time of 3 sec, resulting in a total examination time of 46 sec. Additional scanning parameters were tube voltage 80 kVp, tube current-time product 150 mAs, and section collimation 64 × 1.2 mm with a z-flying focal spot. Patients were instructed to breathe shallowly throughout the scanning. PCT images were reconstructed with a section thickness of 3 mm (increment 2 mm) using a medium-smooth tissue convolution kernel (B20f). Radiation dose parameters derived from the electronically logged patient protocol included a volume CT dose index of 75.76 mGy, and a dose-length product of 911 mGy·cm. The total effective dose for perfusion scanning was 13.6 mSv with a conversion factor of 0.015 mSv/mGy·cm. Dynamic perfusion scanning was followed by a conventional contrast-enhanced portal phase CT extending from the liver dome to the lower margin of the symphysis pubis 60 sec after the administration of an additional 1.2 mL/kg of contrast agent. The total effective dose of the entire CT protocol was 21–29 mSv.

Image analysis

Baseline characteristics including age, sex, and clinical symptoms were obtained from the patients' electronic medical records. Tumor location and size were assessed via operative and/or endoscopic methods. Two radiologists (S.C.H. and S.H.K.) evaluated conventional CT features of the lesions pertaining to enhancement pattern (homogenous vs. heterogeneous), degree (low, iso, or high), shape (endophytic, exophytic, or dumbbell), margin (smooth or lobulated), enhancement of overlying mucosa, lymph node (LN) enlargement, and the presence of necrosis and calcification on portal venous CT, via consensus. The degree of lesion enhancement was compared with that of adjacent normal gastric mucosa. For the LN enlargement, we used a cut-off value of 8mm in short diameter.

Dedicated software (Syngo.via, VA 36A; Siemens) and an application (CT Body Perfusion in Syngo.via) were used for the quantitative analysis of PCT data. An integrated motion-correction algorithm using a non-rigid registration method was applied (14), then peak arterial enhancement was measured in a circular region of interest (ROI) placed in the suprarenal abdominal aorta. Lesion perfusion was calculated using a maximal slope and delayed Patlak models yielding blood flow (BF, mL/100 g/min), blood volume (BV, mL/100 g/min), mean transit time (MTT, sec), and permeability surface value (PS, mL/100 g/min).

Two blinded and independent radiologists (S.C.H. with 3 years of experience in radiology and D.H.L. with 11 years of experience) identified the gastric lesions and manually drew ROIs over the corresponding areas free-hand. The a priori consensus was to draw ROIs on an axial section where the gastric lesion was depicted with the best quality. ROI drawing was done for the entire tumor and for the portion exhibiting the strongest enhancement, avoiding the inclusion of extra-lesional fluid or air (Figs. 2, 3).

Statistical analysis

Continuous variables were expressed as means ± standard deviation, and categorical variables as frequencies or percentages. Data-sets were assessed for normality of distribution using the Shapiro-Wilk test. The chi-square or Fisher's exact test were used to assess the significance of differences in categorical variables between GISTs and non-GISTs, and the Mann-Whitney U test or Student's t-test were used to compare continuous variables. To determine inter-reader agreement for the CT perfusion parameter measurements, intraclass correlation coefficients (ICCs) were calculated for each pair of variables. We considered ICC values greater than 0.81 to represent nearly perfect agreement, and values of 0.61–0.80, 0.41–0.60, and 0.21–0.40 representative of substantial, moderate, and fair agreement, respectively. Values less than 0.21 were considered to indicate slight agreement (15). We also assessed the accuracy of parameters by calculating the non-parametric area under the receiver-operating characteristic (ROC) curve (AUC) with 95% confidence intervals (CI). All statistical analyses

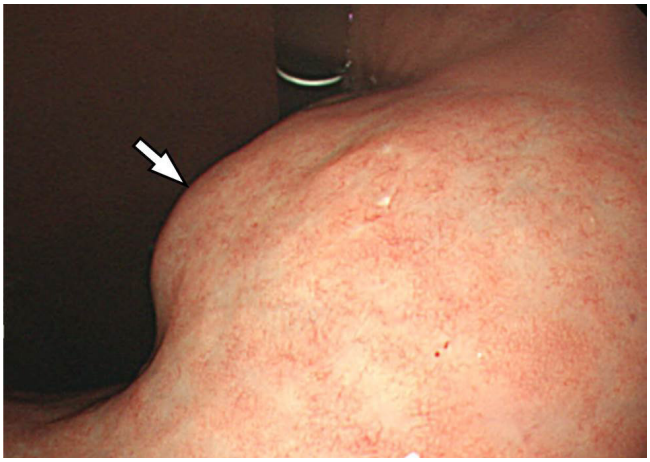

A

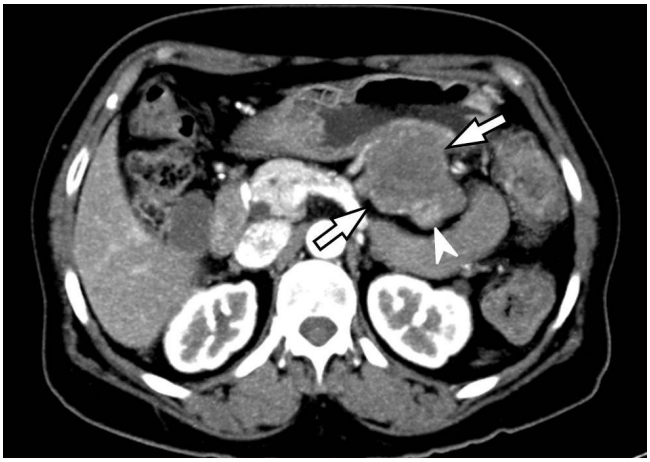

B

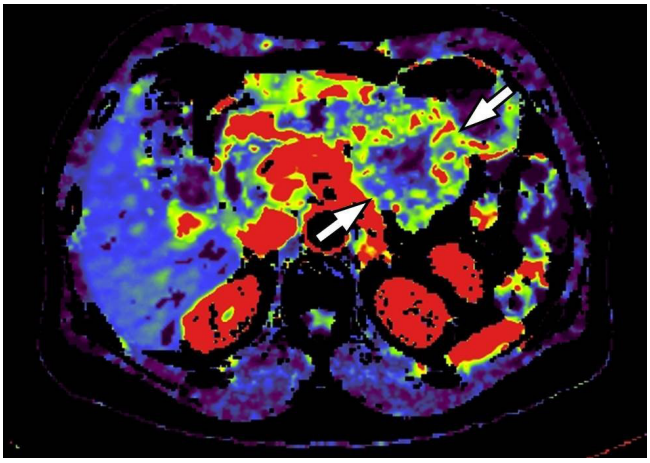

C

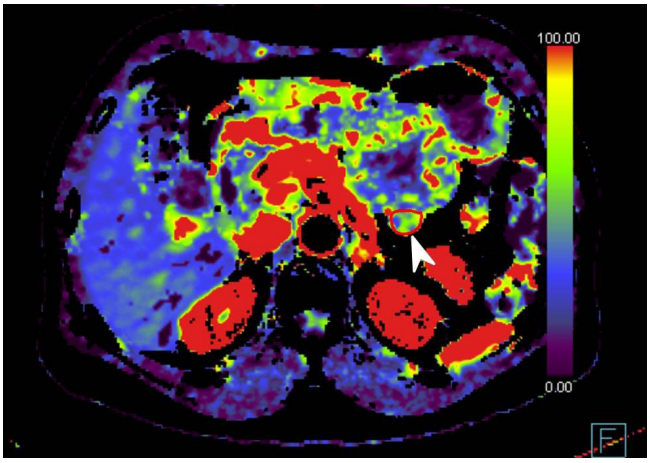

D

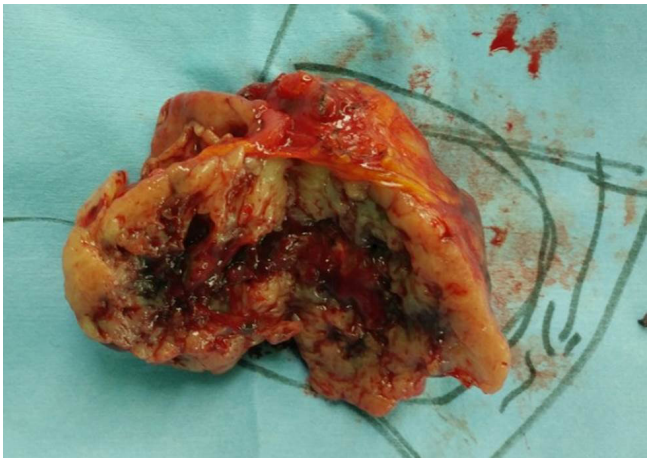

E

Fig. 2. A 68-year-old woman with a high-risk gastrointestinal stromal tumor (GIST). A. Gastroscopic image shows a large subepithelial tumor (arrow) at posterior wall of gastric lower body. B. Maximum intensity projection CT image shows a 6cm large subepithelial tumor (arrows) with internal low attenuation and enhancing portion (arrowhead). C. A color map of permeability surface value demonstrates heterogeneous color signal within the tumor (arrows), suggesting an intra-tumoral heterogeneity. D. Permeability surface value at the strongest enhancing portion (arrowhead) was measured as 75.2 mL/100 g/min. E. Wedge resection was performed and final histopathology confirmed a high-risk GIST with 10 mitosis/50 high-power fields.

were performed using SPSS software (version 22; SPSS Inc., Chicago, Illinois), and $p < 0.05$ was considered statistically significant.

Results

Baseline characteristics

Among the 31 cases, 24 were histologically confirmed as GISTs (4, no risk of malignancy; 11, very low risk; 2, low risk; 5, intermediate risk; and 2, high risk) and 7 were confirmed as benign non-GISTs (3 leiomyomas, 3 schwannomas, and 1 totally necrotic nodule). GISTs were further subcategorized into a no risk to low risk group (including no risk, very low risk, and low risk GISTs) and an intermediate to high risk group (including intermediate risk and high risk GISTs). The malignant potential of GISTs was assessed as very low, low, intermediate, or high on the basis of their mitotic index and size, according to the revised National Institutes of Health consensus criteria (the Joensuu risk criteria) (15). The majority of the tumors were longitudinally located in the upper body (11/31; 35.5%) and transversely located at the anterior wall and greater

A

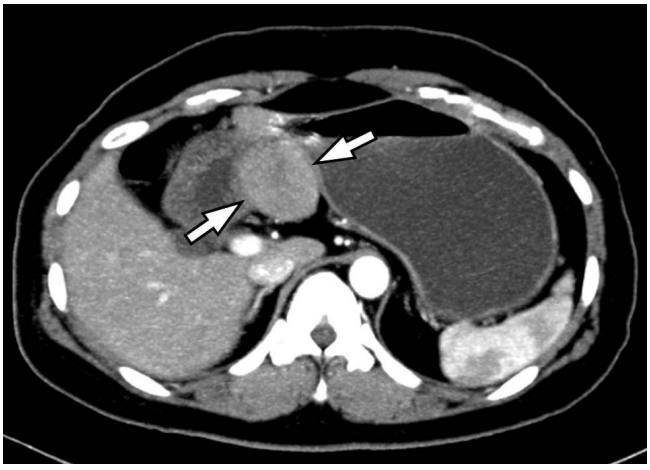

B

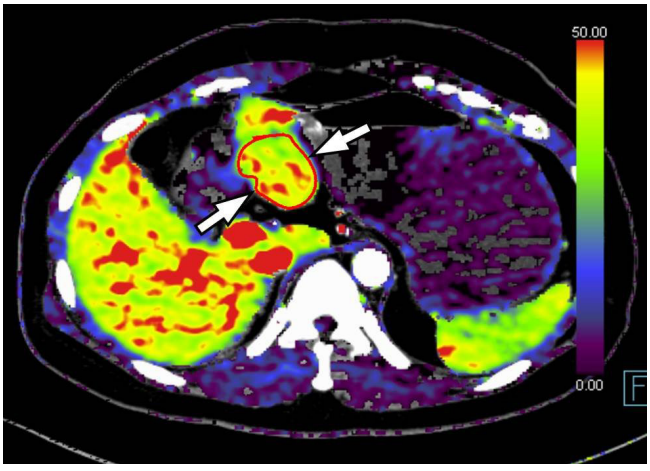

C

D

Fig. 3. A 42-year-old woman with a very low-risk gastrointestinal stromal tumor (GIST). A. Gastroscopic image shows a large subepithelial tumor (arrows) at anterior wall of gastric angle. B. Maximum intensity projection CT image shows a 4.6 cm large subepithelial tumor (arrows) with relatively homogeneous enhancement. C. Permeability surface value at the entire tumor as well as the strongest enhancing portion (arrows) was measured as 42.5 mL/100 g/min. D. Subtotal gastrectomy was performed and final histopathology confirmed a very low-risk GIST with 2 mitosis/50 high-power fields.

curvature of the stomach (9/31; 29.0% each). The median tumor size was 2.8 cm (range 1.5–8.0 cm). There were no significant differences in baseline characteristics between the GIST and non-GIST groups (Table 1).

Conventional CT features

In univariate analysis, the non-GIST group exhibited a high proportion of LN enlargement (28.6% vs. 0%, p = 0.045), and all the positive cases were confirmed as schwannomas. There were no other statistically significant differences in CT features between the two groups (Table 2). Among the 24 GISTs, 17 were assigned to the no risk to low risk group and the remaining 7 were assigned to the intermediate to high risk group, and there were no significant differences in any conventional CT features between these two groups.

Table 1. Baseline Characteristics of GISTs and non-GISTs

	GISTs	Non-GISTs	P value
Age (years)	62.5 ± 8.9	55.1 ± 21.8	0.394
Sex (M:F)	4:20	1:6	1
Tumor size (cm)	3.4 ± 1.7	4.4 ± 1.4	0.089

Data are mean ± standard deviation. P values were calculated using Mann-Whitney U test and Fisher's exact test. GIST=gastrointestinal stromal tumor.

CT perfusion parameters

Among the perfusion parameters, the mean PS in the most strongly enhanced area of GISTs (25.3 ± 23.9 mL/100 g/min) was significantly higher than that of other benign SETs (8.8 ± 8.8 mL/100 g/min) (p = 0.029). There were no significant differences in any other CT perfusion parameters (Figs. 2-5) (Table 3). There were also no significant differences in perfusion parameters between the no risk to low risk GIST group and the intermediate to high risk GIST group.

ICCs indicated nearly perfect reliability for most of the CT perfusion parameters with regard to the entire tumor, except for MTT, which exhibited moderate reliability (BF 0.928, 95% CI 0.853 to 0.965; BV 0.911, 95% CI 0.814 to 0.957; PS 0.953, 95% CI 0.902 to 0.977; MTT 0.468, 95% CI -0.118 to 0.745). For the areas of strongest enhancement, BF and BV ICCs also indicated nearly perfect reliability (BF 0.933, 95% CI 0.861 to 0.968; BV 0.949, 95% CI 0.896 to 0.976). However, PS and MTT ICCs indicated moderate reliability (PS 0.531, 95% CI 0.016 to 0.775; MTT 0.542, 95% CI 0.044 to 0.780) (16).

In ROC analysis of PS in the areas of strongest enhancement, the AUC was 0.774 ± 0.211 (p = 0.03), and sensitivity was 91.7% (22/24) and specificity was 57.1% (4/7) with regard to the diagnosis of GISTs when

Table 2. Statistical Analysis for Conventional CT Features between GISTs and non-GISTs

		GISTs (n=24)	Non-GISTs (n=7)	P value
Enhancement degree	Low	12 (50.0%)	5 (71.4%)	0.605
	Iso	6 (25.0%)	1 (14.3%)	
	High	6 (25.0%)	1 (14.3%)	
Enhancement pattern	Homogeneous	15 (62.5%)	6 (85.7%)	0.379
	Heterogeneous	9 (37.5%)	1 (14.3%)	
Shape	Endophytic	8 (33.3%)	2 (28.6%)	0.549
	Dumbbell	13 (54.2%)	3 (42.9%)	
	Exophytic	3 (12.5%)	2 (28.6%)	
Enhancement of overlying mucosa	Iso	24 (100.0%)	7 (100.0%)	NA
	Hyper	0 (0.0%)	0 (0.0%)	
Necrosis		7 (29.2%)	0 (0.0%)	0.161
Margin	Smooth	16 (66.7%)	2 (28.6%)	0.099
	Lobulated	8 (33.3%)	5 (71.4%)	
Lymph node enlargement		0 (0.0%)	2 (28.6%)	0.045
Calcification		1 (4.2%)	1 (14.3%)	0.406

Data were the number (percentage). P values were calculated using Chi-square or Fisher's exact test. GIST=gastrointestinal stromal tumor, NA=not available. P value in Bold represents a statistical significance.

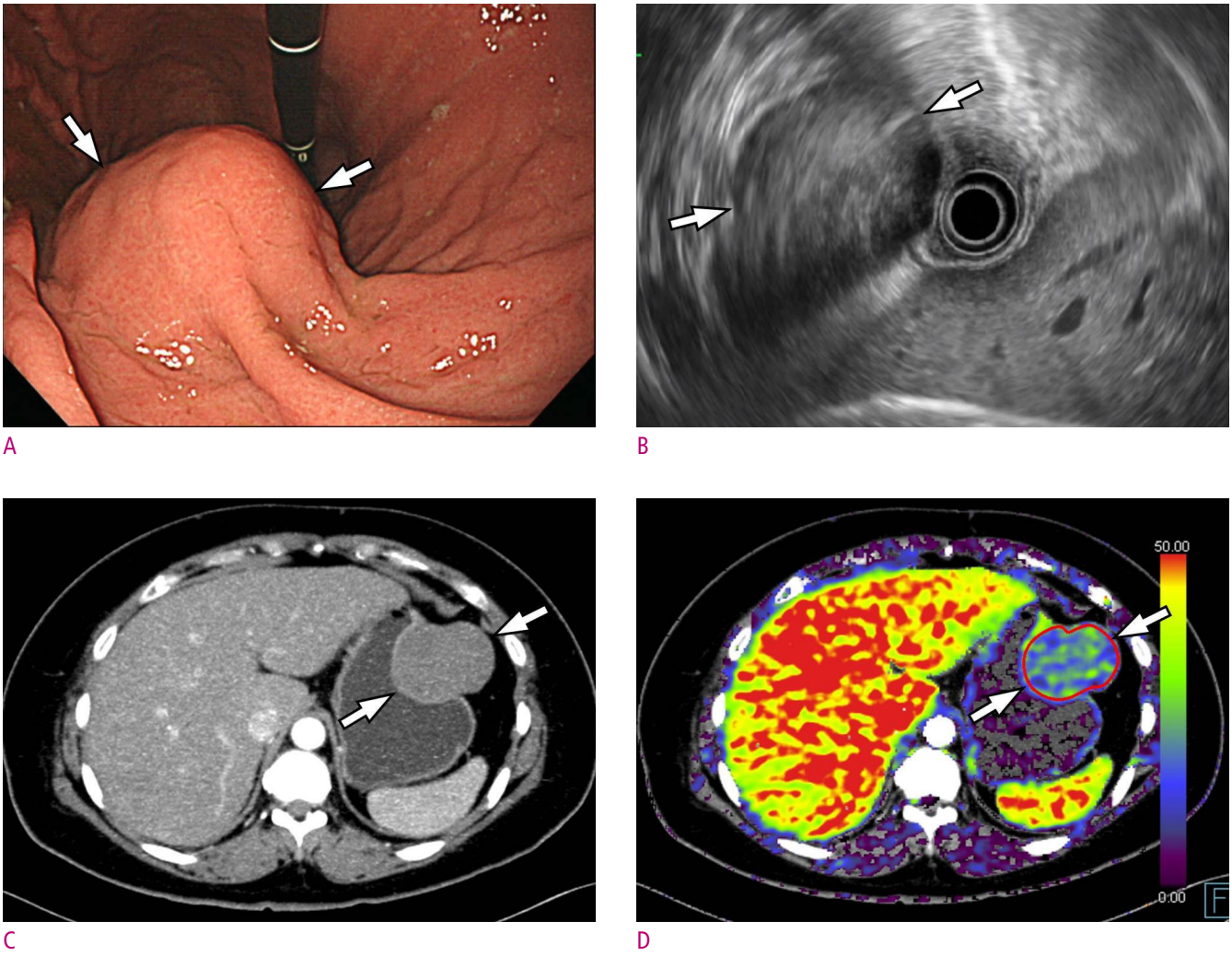

Fig. 4. A 46-year-old woman with gastric schwannoma. A. A gastroscopic image depicts a subepithelial tumor (arrows) at anterior wall of gastric mid-body. B. Endoscopic ultrasonography demonstrates a hypoechoic subepithelial mass (arrows) arose from the 4th proper muscle layer. C. Maximum intensity projection CT image shows a homogeneous low-attenuating mass (arrows) at the corresponding area. D. Permeability surface value at the entire tumor as well as the strongest enhancing portion (arrows) was measured as 20.32 mL/100 g/min. Wedge resection was performed and final histopathology confirmed a gastric schwannoma (not shown).

Table 3. Comparison of CT Perfusion Parameters between GISTs and Non-GISTs

		GISTs (n=24)	Non-GISTs (n=7)	P value
Entire tumor	Blood flow	29.7±14.4	19.6±10.5	0.096
	Blood volume	7.1±3.5	4.5±2.3	0.104
	Mean transit time	13.2±3.8	10.4±5.7	0.141
	Permeability Surface value	22.0±16.2	16.2±5.6	0.695
Strongest enhancing portion	Blood flow	37.5±17.6	26.9±15.7	0.161
	Blood volume	8.6±4.1	5.6±3.0	0.079
	Mean transit time	12.3±5.3	8.8±5.4	0.132
	Permeability Surface value	25.3±23.9	8.8±8.8	0.029

Data are mean ± standard deviation. P values were calculated using Mann-Whitney U test.

P value in Bold represents a statistical significance.

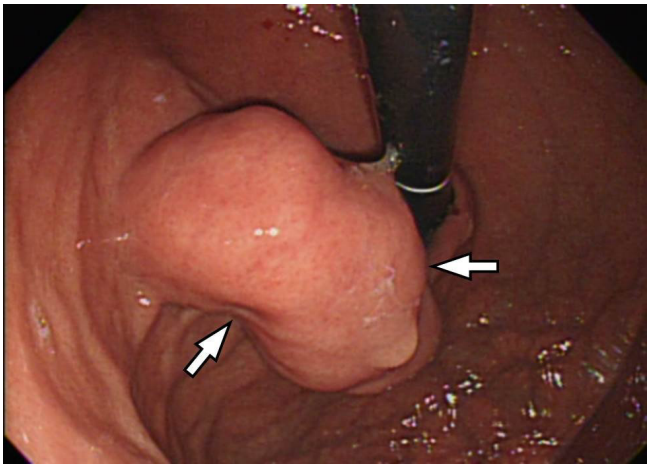

A

B

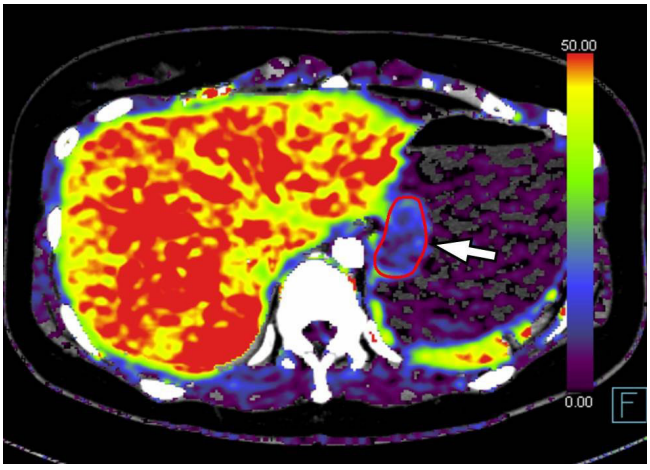

C

D

Fig. 5. A 30-year-old woman with gastric leiomyoma. A. A gastroscopic image depicts a subepithelial tumor (arrows) at gastric cardia adjacent to gastro-esophageal junction. B. Maximum intensity projection CT image shows a homogeneous low-attenuating mass (arrow). C. Permeability surface value at the entire tumor as well as the strongest enhancing portion (arrow) was measured as 6.52 mL/100 g/min. D. Wedge resection was performed and final histopathology confirmed a gastric leiomyoma.

the PS cut-off value was set at 7.17 mL/100 g/min (Fig. 6).

Discussion

In the current study, PS in the areas of strongest enhancement of GISTs was an independently significant CT perfusion parameter with respect to differentiating GISTs from other benign SETs. More specifically, the mean PS of GISTs in the areas of strongest enhancement (25.3 ± 23.9 mL/100 g/min) was significantly higher than that of non-GISTs (8.8 ± 8.8 mL/100 g/min). In addition, although the difference was not statistically significant, BF and BV of GISTs tended to be greater than those of non-GISTs. These results were concordant with previous reports (17, 18). In several previous studies, over-expression of angiogenesis-related factors such as vascular endothelial growth factor and hypoxia-inducible factor 1 alpha was detected in GISTs (17, 18). Furthermore, given the malignant potential of GISTs they may contain more leaky vessels than other benign SETs, leading to higher PS because—theoretically—PS represents the flux of plasma from the intravascular interstitial space to the extravascular interstitial space (9, 13). Therefore, the different microvasculature and vessel permeability of GISTs

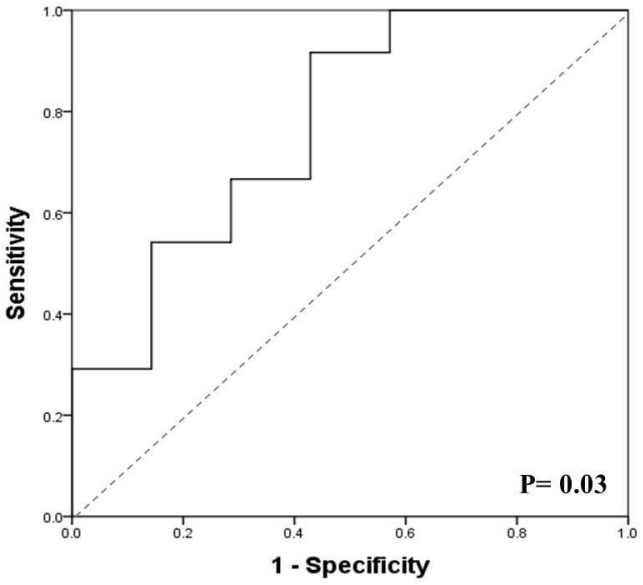

Fig. 6. Result of receiver operating characteristic curve (ROC) analysis. ROC analysis of permeability surface value of the strongest enhancing area to predict GIST reveals an area under the curve of 0.774 (95% confidence interval, 0.563–0.985, P=0.03).

may be responsible for the higher perfusion values they exhibit compared to non-GISTs.

Other than CT perfusion values, LN enlargement was the only significant conventional CT feature pertaining to differentiation between GISTs and non-GISTs. None of the GISTs were associated with lymphadenopathy, whereas 2 of the 7 benign SETs were associated with LN enlargement. Both of these lesions were confirmed to be schwannomas. This result is also concordant with previous reports (3, 6). According to Choi et al. (3), gastric schwannomas tend to be associated with LN enlargement. Though the precise pathophysiological mechanisms involved in the frequent lymphadenopathy associated with schwannoma have not been investigated, the authors assume that a lymphophilic cytokine or cytokines may induce LN enlargement in this context because schwannoma is frequently accompanied by perilesional lymphoid cuffing at the periphery of the lesion (3). Therefore, we believe that the combined use of the presence of LN enlargement and lower PS value may increase the accuracy of gastric schwannoma diagnosis.

Contrary to our expectation that greater malignant potential in high-risk GISTs may result in higher perfusion values than in low-risk GISTs, there were no significant differences in CT perfusion parameters or conventional CT features between high-risk and low-risk GISTs. The small sample sizes in the study may have been responsible for these non-significant results. A future study including a large number of patients is required, to clarify these unexpected results.

High inter-observer and intra-observer variability are known limitations of the utilization of CT to investigate perfusion. In the present study however, ICC values for CT perfusion parameters between the two assessors were high, indicating near perfect or moderate reliability. We believe that the use of a motion correction algorithm may be responsible for such high reproducibility of CT perfusion values. Because the determination of perfusion via CT requires a long image acquisition time, the use of a motion correction algorithm could be considered essential. Goetti et al. (19) reported that without a motion correction algorithm quantitative assessment was impossible due to respiratory motion in approximately 30% of patients with liver lesions.

The current study had several limitations. The most limiting factors were that it was a single-center study and it only included a small number of participants (N = 31). However, we believe that the number of patients may be sufficient for a preliminary study investigating the use of PCT for the differentiation of gastric SETs. Although not significant in the present study, the higher values for most of the CT perfusion parameters in the GIST group is promising, and emphasizes the need for a multi-center study with a larger number of patients. Another limitation was reliance on the radiologist's subjective opinion with regard to the area with the strongest enhancement, which may have led to reduced reproducibility. Notably in this respect, the ICC of the PS of the area of strongest enhancement was lower than the ICC of the PS of the entire tumor. Lastly, despite the availability of various analytical systems for determining perfusion via CT, the present study was conducted with only one model from one manufacturer. Because our results were based on the delayed Patlak and maximum slope models, other analytical methods such as deconvolutional models may yield different results (20, 21).

In conclusion, perfusion parameters determined via PCT in patients with gastric SET were useful for the differentiation of GISTs from other benign SETs, as PS

values in GISTs were significantly higher than those of non-GIST SETs.

ORCID: Seungchul Han: https://orcid.org/0000-0002-7276-0370; Se Hyung Kim: https://orcid.org/0000-0001-8664-0356; Dong Ho Lee: https://orcid.org/0000-0001-8983-851X

Acknowledgments

This research was supported by Basic Science Research Program through the National Research Foundation of Korea [NRF] funded by the Ministry of Science, ICT& Future Planning (NRF-2021R1F1A1046393) and from the Seoul National University Hospital Research Fund No. 03-2023-0340.

References

1. Hedenbro JL, Ekelund M, Wetterberg P. Endoscopic diagnosis of submucosal gastric lesions. The results after routine endoscopy. Surg Endosc 1991;5:20-23.
2. Polkowski M. Endoscopic ultrasound and endoscopic ultrasound-guided fine-needle biopsy for the diagnosis of malignant submucosal tumors. Endoscopy 2005;37:635-645.
3. Choi YR, Kim SH, Kim SA, Shin CI, Kim HJ, Kim SH, et al. Differentiation of large (>/= 5 cm) gastrointestinal stromal tumors from benign subepithelial tumors in the stomach: radiologists' performance using CT. Eur J Radiol 2014;83:250-260.
4. Miettinen M, Lasota J. Gastrointestinal stromal tumors: pathology and prognosis at different sites. Semin Diagn Pathol 2006;23:70-83.
5. Nilsson B, Bumming P, Meis-Kindblom JM, Oden A, Dortok A, Gustavsson B, et al. Gastrointestinal stromal tumors: the incidence, prevalence, clinical course, and prognostication in the preimatinib mesylate era--a population-based study in western Sweden. Cancer 2005;103:821-829.
6. Choi JW, Choi D, Kim KM, Sohn TS, Lee JH, Kim HJ, et al. Small submucosal tumors of the stomach: differentiation of gastric schwannoma from gastrointestinal stromal tumor with CT. Korean J Radiol 2012;13:425-433.
7. Yang HK, Kim YH, Lee YJ, Park JH, Kim JY, Lee KH, et al. Leiomyomas in the gastric cardia: CT findings and differentiation from gastrointestinal stromal tumors. Eur J Radiol 2015;84:1694-1700.
8. Kim DH, Kim SH, Im SA, Han SW, Goo JM, Willmann JK, et al. Intermodality comparison between 3D perfusion CT and 18F-FDG PET/CT imaging for predicting early tumor response in patients with liver metastasis after chemotherapy: preliminary results of a prospective study. Eur J Radiol 2012;81:3542-3550.
9. Kim SH, Kamaya A, Willmann JK. CT perfusion of the liver: principles and applications in oncology. Radiology 2014;272:322-344.
10. Lv WF, Han JK, Cheng DL, Zhou CZ, Ni M, Lu D. CT Perfusion Imaging Can Predict Patients' Survival and Early Response to Transarterial Chemo-Lipiodol Infusion for Liver Metastases from Colorectal Cancers. Korean J Radiol 2015;16:810-820.
11. Lee DH, Kim SH, Joo I, Han JK. CT Perfusion evaluation of gastric cancer: correlation with histologic type. Eur Radiol 2018;28:487-495.
12. Lundsgaard Hansen M, Fallentin E, Lauridsen C, Law I, Federspiel B, Baeksgaard L, et al. Computed tomography (CT) perfusion as an early predictive marker for treatment response to neoadjuvant chemotherapy in gastroesophageal junction cancer and gastric cancer--a prospective study. PLoS One 2014;9:e97605.
13. Zhang H, Pan Z, Du L, Yan C, Ding B, Song Q, et al. Advanced gastric cancer and perfusion imaging using a multidetector row computed tomography: correlation with prognostic determinants. Korean J Radiol 2008;9:119-127.
14. Gordic S, Puippe GD, Krauss B, Klotz E, Desbiolles L, Lesurtel M, et al. Correlation between Dual-Energy and Perfusion CT in Patients with Hepatocellular Carcinoma. Radiology 2016;280:78-87.
15. Joensuu H. Risk stratification of patients diagnosed with gastrointestinal stromal tumor. Hum Pathol 2008;39:1411-1419.
16. Landis JR, Koch GG. The measurement of observer agreement for categorical data. Biometrics 1977;33:159-174.
17. Nakayama T, Cho YC, Mine Y, Yoshizaki A, Naito S, Wen CY, et al. Expression of vascular endothelial growth factor and its receptors VEGFR-1 and 2 in gastrointestinal stromal tumors, leiomyomas and schwannomas. World J Gastroenterol 2006;12:6182-6187.
18. hen WT, Huang CJ, Wu MT, Yang SF, Su YC, Chai CY. Hypoxia-inducible factor-1alpha is associated with risk of aggressive behavior and tumor angiogenesis in gastrointestinal stromal tumor. Jpn J Clin Oncol 2005;35:207-213.

19. Goetti R, Reiner CS, Knuth A, Klotz E, Stenner F, Samaras P, et al. Quantitative perfusion analysis of malignant liver tumors: dynamic computed tomography and contrast-enhanced ultrasound. Invest Radiol 2012;47:18-24.
20. Goh V, Halligan S, Bartram CI. Quantitative tumor perfusion assessment with multidetector CT: are measurements from two commercial software packages interchangeable? Radiology 2007;242:777-782.
21. Kanda T, Yoshikawa T, Ohno Y, Kanata N, Koyama H, Takenaka D, et al. CT hepatic perfusion measurement: comparison of three analytic methods. Eur J Radiol 2012;81:2075-2079.

관류 CT가 위에서 위장관기질종양과 다른 양성 상피하종양을 구분하는데 유용한가?

한승철[1], 김세형[2,3], 이동호[2,3]

[1]삼성서울병원 영상의학과
[2]서울대학교병원 영상의학과
[3]서울대학교 의학연구센터 방사선의학연구소

목 적: 위에서 위장관기질종양을 다른 양성 상피하종양과 감별함에 있어 관류 CT의 진단능을 평가하고자 한다.
대상과 방법: 수술로 위 상피하종양으로 진단된 31명의 환자가 80kVp 전압 다중채널 CT를 이용한 관류 CT를 시행하였다. 두 명의 영상의학과 의사가 종양의 균질도 및 조영증강 정도를 포함한 다양한 고식적 CT 소견을 분석하였다. 또 다른 두 명의 영상의학과 의사가 관류 CT에서 종양의 혈류량, 혈류 용적, 혈류 평균통과시간, 투과값을 독립적으로 계산하였다. 위장관기질종양와 양성 상피하종양의 CT 소견 및 관류 지표들의 차이를 통계 분석하였다. 관류 지표의 진단능은 수신자조작특성 분석을 이용하여 평가하였다.
결 과: 병리학적 검사에서 24명의 환자가 위장관기질종양으로 진단되었고, 나머지 7명 중 3명은 평활근종, 3명은 신경초종, 1명은 완전괴사종괴로 진단되었다. 고식적 CT 소견 중 림프절 종대 유무만이 유일하게 위장관기질종양 (0/24, 0%)과 비위장관기질종양 (2/7, 28.6%)간에 차이를 보였다 (p=0.045). 관류 CT 지표 중에서는 가장 조영증강이 잘되는 부위에서 측정한 평균 투과값이 위장관기질종양 (25.3 ± 23.9 mL/100g/min) 에서 다른 양성 상피하종양 (8.8 ± 8.8 mL/100 g/min)보다 유의하게 컸다 (p=0.029). 수신자조작특성 분석 결과, 투과값 컷오프를 7.17 mL/100 g/min으로 설정하였을 때, 수신자조작특성 곡선하 면적은 0.774 (p=0.03), 민감도는 91.7%, 특이도는 57.1%였다.
결 론: 관류 CT는 위에서 위장관기질종양을 다른 양성 상피하종양과 감별하는데 유용하게 사용될 수 있으며, 특히 위장관기질종양이 다른 양성 상피하종양보다 유의하게 높은 투과값을 보였다.